Mode coupling in lead zirconate titanate/epoxy 1–3 piezocomposite rings

S. W. Or[a] and H. L. W. Chan[b]
Department of Applied Physics and Materials Research Centre, The Hong Kong Polytechnic University, Hunghom, Kowloon, Hong Kong

(Received 18 April 2001; accepted for publication 26 July 2001)

Lead zirconate titanate (PZT)/epoxy 1–3 piezocomposite rings were fabricated with PZT volume fractions ϕ ranging from 0.82 to 0.94 and with a small epoxy width of 77 μm in order to investigate their resonance characteristics and to reveal the mode coupling. Four major resonance modes were observed, namely the coupled longitudinal-thickness f_H and lateral f_{L1} and f_{L2} mode resonances of individual PZT elements inside the rings as well as the radial f_R and wall-thickness f_W mode resonances of the whole rings. No stopband resonances were observed in the frequency range of 1 to 10 MHz. f_H was found to increase linearly with the decrease in element height while f_{L1} and f_{L2} remained constant. When the height and width of the elements became comparable, coupling of f_H with f_{L1} and f_{L2} occurred. The observed f_H, f_{L1}, and f_{L2} for all samples agreed with those calculated by the mode-coupling theory. f_R and f_W were almost independent of the ring thickness but increased as ϕ increased. A guide of operating f_H in the rings without causing mode coupling was presented to optimize the composite structure for transducer design. © *2001 American Institute of Physics.* [DOI: 10.1063/1.1405139]

I. INTRODUCTION

1–3 piezocomposites, consisting of one dimensionally connected piezoceramic elements embedded in a three dimensionally connected passive polymer matrix, have been an important breakthrough in overcoming the drawbacks of piezoceramics for hydrophones in underwater sonar with operating frequencies below 40 kHz as well as for pulse–echo transducers and undiced transducer arrays in medical ultrasonic imaging functioning in the megahertz frequency range.[1–11] The underwater applications require high hydrophone receiving sensitivity, which is achieved by eliminating the response from an incident acoustic pressure applied to the edges of the hydrophone due to a buckling effect and by acoustically matching the impedance between the hydrophone and water. The most important consideration in medical ultrasound is to optimally match the acoustic impedance of the transducer to that of the human tissue in order to achieve high sensitivity, wide bandwidth, and low lateral mode interference. In both cases, disk or plate-shaped composites with relatively low volume fractions of ceramic well below 0.8 are typically used at frequencies near their thickness resonances. Accordingly, the resonance characteristics of these composites have been studied,[5,7–10] and a good understanding of mode coupling has been established.

For solid-state driving or actuation purposes, however, little information is available on using 1–3 type piezocomposites where high volume fraction of ceramic (>0.8) should be adopted. Ring-shaped lead zirconate titanate (PZT) piezoceramics have been used extensively in various low frequency (<100 kHz) ultrasonic devices such as ultrasonic motors, welding transducers, piezoelectric transformers, etc., and their resonance characteristics have been reported elsewhere.[12] For some dedicated applications such as high frequency ultrasonic wire bonding of microelectronic packages, thickness-driven, axial mode transducers operating at a few hundred kilohertz are of prime importance. As PZT (typically hard PZT) rings used in state-of-the-art transducers have many nonaxial modes at these frequencies, they will couple with the desired axial mode of the transducer and cause significant degradation of its performance. By using 1–3 piezocomposite rings, the mode-coupling problem can be greatly alleviated, and pure axial mode can be attained.[13–17] Therefore, in this work, we aim at fabricating PZT/epoxy 1–3 piezocomposite rings and determining their resonance characteristics.

II. FABRICATION OF 1–3 PIEZOCOMPOSITE RINGS

The 1–3 piezocomposite rings were fabricated using the dice-and-fill technique.[1,7,13] PKI804 PZT rings (12.7 mm outer diameter, 5.0 mm inner diameter, and 2.5 mm thickness) and Araldite LY5210/HY2954 epoxy were used as the active and passive phases in the 1–3 structure, respectively. Two sets of equally spaced, parallel grooves were cut in the PZT rings in orthogonal directions using a Disco DAD 341 automatic dicing saw equipped with a diamond saw blade of 70 μm thickness. However, the grooves did not go right through the ring thickness. Approximately 0.19 mm of PZT was allowed to remain on the base so that the whole ring structure could be retained after cutting. Due to blade vibration, the resulting grooves in the ring were about 77 μm wide as measured by a traveling microscope. Thus, by applying a different number of cuts (5, 7, 9, 11, 13, and 15 cuts/direction) to the PZT rings, piezocomposite rings with different PZT element widths L of 2.03, 1.50, 1.19, 0.98, 0.83, and 0.71 mm and with different ϕ values of 0.94, 0.91,

[a]Also at: ASM Assembly Automation Ltd., 4/F, Watson Center, 16 Kung Yip Street, Kwai Chung, Hong Kong; electronic mail: swor@ieee.org
[b]Author to whom all correspondence should be addressed; electronic mail: apahlcha@polyu.edu.hk

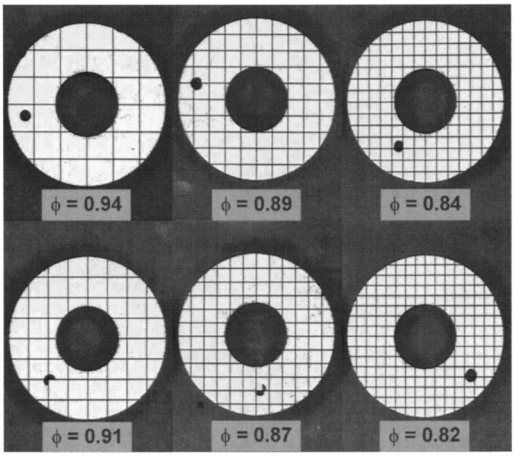

FIG. 1. Fabricated PKI804/Araldite LY5210/HY2954 piezocomposite rings are shown. The black epoxy dot is a polarity marking to indicate the anode (connected to positive voltage during poling).

0.89, 0.87, 0.84, and 0.82 were obtained, respectively (Fig. 1). Due to the fineness of the grooves, filling of epoxy under a vacuum was carried out. The cured composite rings were lapped to grind off the PZT base and to obtain a pair of flat and parallel surfaces. It was found that a thickness of 2.30 ± 0.02 mm could generally be obtained after lapping.

III. RESONANCE MODES IN 1–3 PIEZOCOMPOSITE RINGS

Resonance modes of a 1–3 piezocomposite ring can be classified into two main categories as follows.

(1) Characteristic resonances of individual PZT elements inside the ring comprise the first category.
   (a) The coupled longitudinal-thickness mode resonance f_H, which is essentially determined by the height H of the PZT elements, is the mode of practical interest in ultrasonic transducers as it corresponds to the thickness mode resonance f_t of the composite ring.
   (b) The coupled lateral mode resonances f_{L1} and f_{L2} are mainly determined by the width L of the PZT elements with square cross section.

   When the composite ring is thick, the PZT elements are tall thin bars, and f_H is well separated from f_{L1} and f_{L2}. When the elements approach the shape of a cube, coupling of these resonance modes occurs. This mode-coupling effect can be predicted using the mode-coupling theory,[7,8] which will be described in the next section.
(2) Cooperative resonances of the whole ring comprise the second category.
   (a) The radial f_R and wall-thickness f_W mode resonances are the lateral resonances of the composite ring as a whole and are usually the two low frequency resonance modes in a thin ring. They are essentially determined by the mean diameter and wall-thickness of the ring, respectively.
   (b) The stopband resonances f_{S1} and f_{S2} result from the periodic structure of the composite and occur at frequencies near where scattering of laterally propagating shear waves in the epoxy matrix from the planes of the regular spaced PZT elements occur. They are related to the lateral periodicity d (one epoxy width d_P + one element width L) if composites have low values of ϕ (<0.25) with large d_P.[7,9,10] In contrast, they are mainly determined by d_P for composites possessing relatively high values of ϕ with sufficiently small d_P.[9,10,18] The composite rings fabricated in the present work belong to the latter case.

IV. THE MODE-COUPLING THEORY

Consider a square parallelepiped with width L in the x and y directions and height H in the z direction. This parallelepiped is essentially equivalent to an individual PZT element inside a 1–3 composite with its z axis taken as the poling axis and with both square surfaces normal to the z axis being entirely electroded. The frequency equation of this parallelepiped can be expressed as[7,8]

$$[f^2-f_a^2(1-\gamma)]\{f^4-[f_a^2(1+\gamma)+f_b^2]f^2 + f_a^2f_b^2(1+\gamma-2\alpha^2)\}=0, \tag{1}$$

where

$$f_a=\frac{1}{2L}\sqrt{\frac{c_{11}}{\rho}}, \tag{2}$$

and

$$f_b=\frac{1}{2H}\sqrt{\frac{c_{33}}{\rho}}, \tag{3}$$

are the uncoupled lateral and longitudinal-thickness resonance frequencies, respectively; $\gamma=c_{12}/c_{11}$ and $\alpha=c_{13}/\sqrt{c_{11}c_{33}}$ are the coupling constants; c_{11}, c_{12}, c_{13}, and c_{33} are the elastic stiffness constants; and ρ is the density. Equation (1) can be factorized into a quadratic and a biquadratic equation as follows.

(1) The quadratic equation is
$$f^2-f_a^2(1-\gamma)=0. \tag{4}$$
It gives two solutions in which the one with negative root is discarded for physical reasons, leaving only the positive one as
$$f_{L2}=f_a\sqrt{1-\gamma}=\frac{1}{2L}\sqrt{\frac{c_{11}-c_{12}}{\rho}}. \tag{5}$$
f_{L2} is called the coupled lower lateral resonance frequency.
(2) The biquadratic equation is
$$f^4-[f_a^2(1+\gamma)+f_b^2]f^2+f_a^2f_b^2(1+\gamma-2\alpha^2)=0, \tag{6}$$

or

$$f_{\pm}=\frac{1}{\sqrt{2}}\sqrt{f_a^2\left[(1+\gamma)+\left(\frac{G}{\Re}\right)^2\right]\pm\sqrt{f_a^4\left[(1+\gamma)+\left(\frac{G}{\Re}\right)^2\right]^2-4\left(\frac{G}{\Re}\right)^2 f_a^4(1+\gamma-2\alpha^2)}}, \tag{7}$$

where $G=L/H$ is the configuration ratio and $\Re=\sqrt{c_{11}/c_{33}}$ is the coupling constant. Equation (7) has two solutions f_+ and f_-, which give two frequency branches: upper f_+ and lower f_-. The coupled longitudinal-thickness f_H and upper lateral f_{L1} resonance frequencies are governed by these two frequency branches in terms of G.

Table I shows the material parameters of PKI804 PZT.[13,19] Hence, the theoretical curves of the uncoupled [Eqs. (2) and (3)] and coupled [Eqs. (5) and (7)] resonance frequencies at different G can be derived using parameters with superscripts E and D for the short- and open-circuit conditions, respectively. The calculated curves will be compared with experimental results in a later section.

V. THINNING TEST

Thinning test was carried out to study the resonance characteristics of the composite rings. It involves lapping each composite sample to different thicknesses in steps and at each thickness applying a thin silver layer of 5 to 10 μm (G3691 quick drying silver paint from Agar Scientific Ltd. in U.K.) on the two major surfaces to form electrodes and then measuring the electrical impedance spectrum using a HP 4194A impedance analyzer. It should be noted that the measured series resonance frequency was compared with the theoretical predictions calculated using the short-circuit (constant E) parameters. The measured parallel resonance frequency was compared with the theoretical predictions deduced using the open-circuit (constant D) parameters. f_H of the PZT elements is a piezoelectric stiffened mode while the other resonance modes are unstiffened modes.

VI. RESULTS AND DISCUSSION

A. Characteristic resonances of individual PZT elements

Figure 2 shows the thinning test results of a composite ring with $\phi=0.82$ and $L=0.71$ mm. The electrical impedance spectrum of the ring with $H=2.30$ mm ($G=0.31$) is plotted in Fig. 2(a). Guided by the mode-coupling theory, the strongest resonance mode at 0.93 MHz is identified as f_H. The mode at about 2.70 MHz is its third harmonic and is labeled as $3f_H$ since it appears at about three times f_H. Even harmonics are not expected to be observed because the applied electric field has opposite polarity on the two faces of the sample. The two lateral modes f_{L1} and f_{L2} are weak resonances found at 3.73 MHz and 2.48 MHz, respectively. They are often mixed with other high frequency resonances. For example, f_{L2} has merged with $3f_H$ in Fig. 2(a). Besides, there are several weak resonances above f_{L1} and f_{L2}. These may be other lateral modes, which arise from the PZT elements with smaller lateral sizes L such as those elements located near the inner and outer circumferences of the ring as shown in Fig. 1. Moreover, the two small resonances appeared in the lower frequency band of 75 kHz and 306 kHz are f_R and f_W of the whole composite ring, respectively. Detailed behavior of these modes will be discussed later. When the sample is subsequently thinned down [Figs. 2(b)–2(d)], f_H increases accordingly while f_{L1} and f_{L2} stay quite constant. Also, $3f_H$ increases at approximately three times the rate of f_H. If there is no other resonance close to f_{L1} and f_{L2}, the resonance peaks associated with them will be very weak and sometimes even disappear [Fig. 2(b)]. For $H<0.95$ mm ($G>0.75$), f_H starts to couple with f_{L2} [Fig. 2(c)] and later continues to merge with the subsequent lateral modes [Fig. 2(d)], thereby forming a strong but complex resonance mode covering a broad range of frequency. Consequently, f_{L2} serves to impose an upper frequency bound where mode coupling begins.

The general behaviors of f_H, as well as f_{L1} and f_{L2}, at different sample thicknesses for the remaining five batches of composite rings with ϕ values of 0.84, 0.87, 0.89, 0.91, and 0.94 are quite similar to each other and also to the one with $\phi=0.82$. The corresponding spectra for the electrical impedance are shown in Figs. 3–7. The observed results are summarized as follows.

(1) For the sample with $\phi=0.84$ and $L=0.83$ mm (Fig. 3), the initial thickness of the composite is $H=2.31$ mm ($G=0.36$) [Fig. 3(a)]. A clean f_H is observed at 0.93 MHz, then no other resonance is detected until f_{L2} appears at 2.22 MHz. Resonance modes following f_{L2} include other high frequency lateral modes, $3f_H$ (that has mixed with these lateral modes at ~2.80 MHz), and f_{L1} (3.35 MHz). All these lateral resonances are found at frequencies lower than those of the sample with $\phi=0.82$ due to an increment of L from 0.71 to 0.83 mm. When H is reduced, f_H and $3f_H$ rise almost linearly while f_{L1} and f_{L2} remain nearly unchanged [Figs. 3(b)–3(c)]. Coupling of f_H with f_{L2}, as well as the subsequent lateral modes, occurs at $H<1.05$ mm ($G>0.79$) [Fig. 3(c)].

(2) For the sample with $\phi=0.87$ and $L=0.98$ mm (Fig. 4), f_H, $3f_H$, and f_{L1} are found at 0.94 MHz, 2.78 MHz, and 2.96 MHz, respectively for $H=2.31$ mm ($G=0.42$) [Fig. 4(a)]. f_{L2} is not observed because of no nearby resonances but reappears at 1.92 MHz when the

TABLE I. Material parameters of PKI804 PZT[a] are shown.

ρ (kg/m^3) = 7700	c_{11}^E (GPa) = 135.3
c_{11}^D (GPa) = 142.7	c_{12}^E (GPa) = 48.2
c_{12}^D (GPa) = 55.6	c_{13}^E (GPa) = 61.5
c_{13}^D (GPa) = 56.6	c_{33}^E (GPa) = 131.1
c_{33}^D (GPa) = 153.0	

[a]See Refs. 13 and 19.

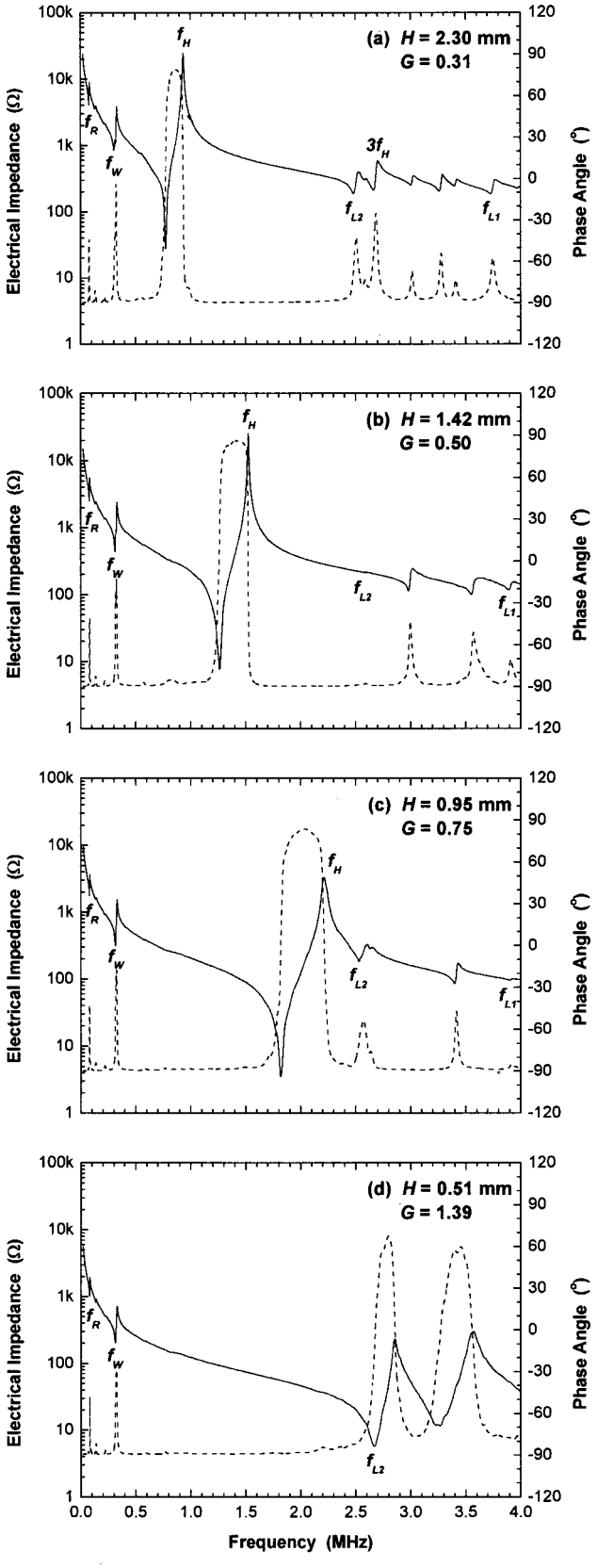

FIG. 2. Electrical impedance (solid line) and phase angle (dot line) versus frequency plots for composite ring with $\phi=0.82$ and $L=0.71$ mm at different thicknesses are shown.

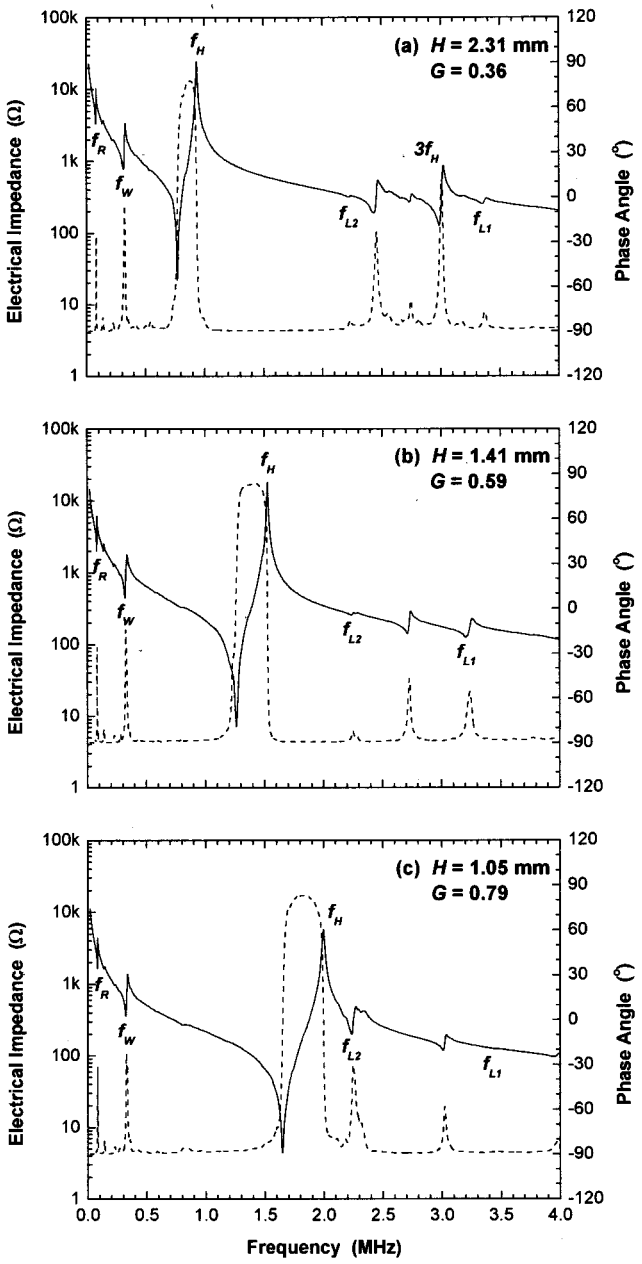

FIG. 3. Electrical impedance (solid line) and phase angle (dot line) versus frequency plots for composite ring with $\phi=0.84$ and $L=0.83$ mm at different thicknesses are shown.

sample is thinned down to 1.70 mm ($G=0.58$) [Fig. 4(b)]. Clearly, the lateral mode resonances, including f_{L1} and f_{L2}, have lower frequencies as compared to the previous batches, but f_H is similar. It increases continuously in response to the thinning process and tends to couple with f_{L2} at $H=1.26$ mm ($G=0.78$) [Fig. 4(c)].

(3) For the sample with $\phi=0.89$ and $L=1.19$ mm (Fig. 5), f_H and $3f_H$ are clearly observed at 0.94 and 2.89 MHz when $H=2.31$ mm ($G=0.52$), and they increase with decreasing sample thickness. Both f_{L1} and f_{L2} remain quite stationary at lower frequencies of 2.42 MHz and

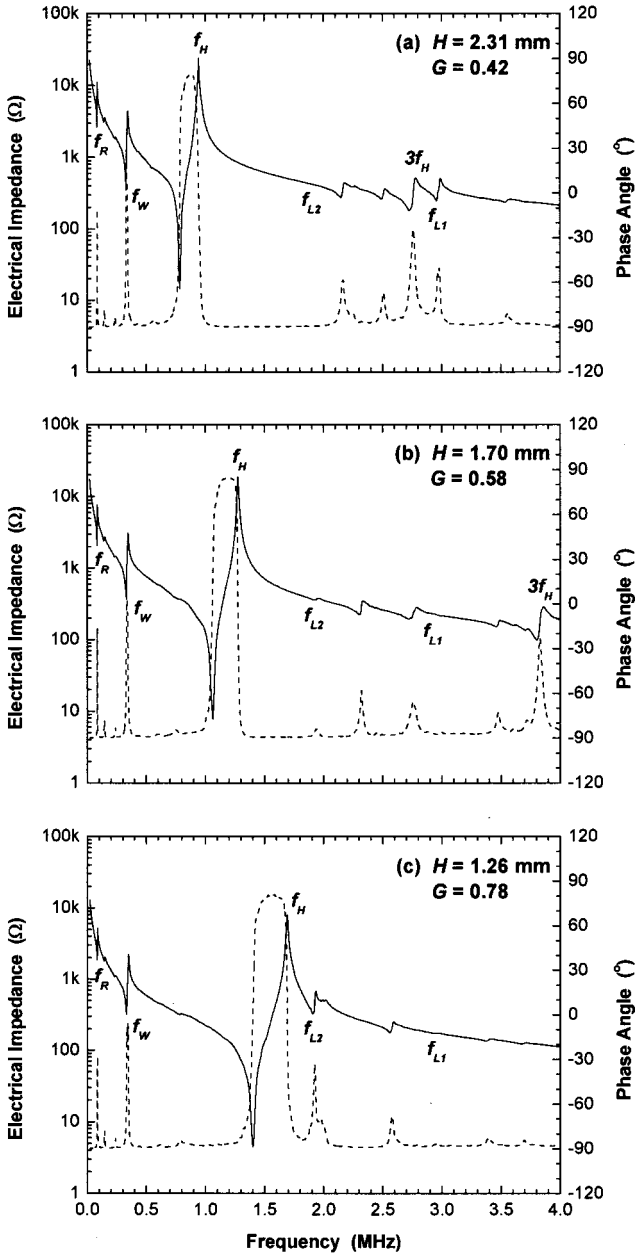

FIG. 4. Electrical impedance (solid line) and phase angle (dot line) versus frequency plots for composite ring with $\phi=0.87$ and $L=0.98$ mm at different thicknesses are shown.

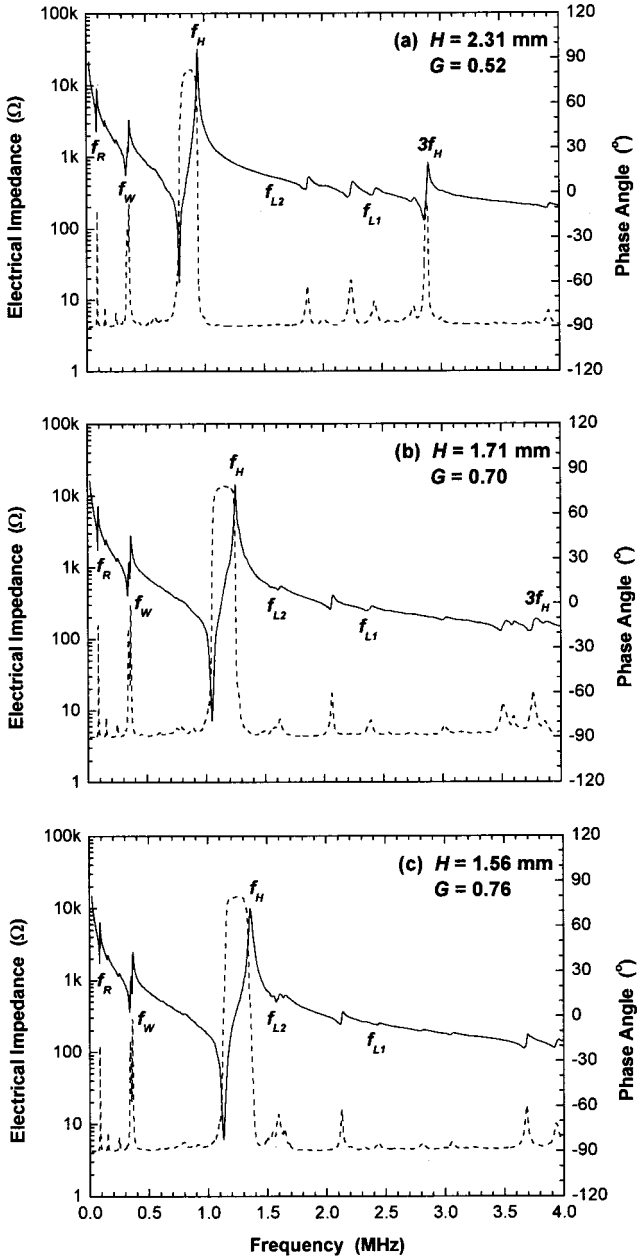

FIG. 5. Electrical impedance (solid line) and phase angle (dot line) versus frequency plots for composite ring with $\phi=0.89$ and $L=1.19$ mm at different thicknesses are shown.

1.61 MHz, respectively. Also, merging of f_H with f_{L2} results at a comparatively larger thickness of $H=1.56$ mm ($G=0.76$) [Fig. 5(c)].

(4) For the sample with $\phi=0.91$ and $L=1.50$ mm (Fig. 6), there are no major changes in f_H (0.94 MHz) and $3f_H$ (2.83 MHz) at $H=2.31$ mm ($G=0.65$). However, the operation bandwidth of f_H is even smaller since f_{L2} is detected at a frequency as low as 1.30 MHz and f_{L1} at 1.87 MHz. The corresponding sample thickness of f_H that starts to couple with f_{L2} is $H<2.01$ mm ($G>0.75$) [Fig. 6(b)].

(5) For the sample with $\phi=0.94$ and $L=2.03$ mm (Fig. 7), mode coupling is apparent, and complex peaks are found even for sample as thick as 2.31 mm ($G=0.88$) [Fig. 7(a)]. Nevertheless, the mode-coupling theory still can provide a good guide for locating the position of f_H, f_{L1}, and f_{L2}.

The observed f_H, f_{L1}, and f_{L2} for all composite samples at different thicknesses are plotted in Fig. 8 as the short- and open-circuit cases together with the mode-coupling theory predictions, and good agreements are obtained. The small offsets from the theoretical curves may be owed to the clamping effect imposed on the PZT elements by the epoxy matrix. At $G>0.8$, significant mode coupling of f_H with f_{L1} and f_{L2} occurs, so the data exhibit some scattering. According to the predictions, f_H will decouple with f_{L1} and f_{L2} for $G>1.5$. However, it is not the case in practice

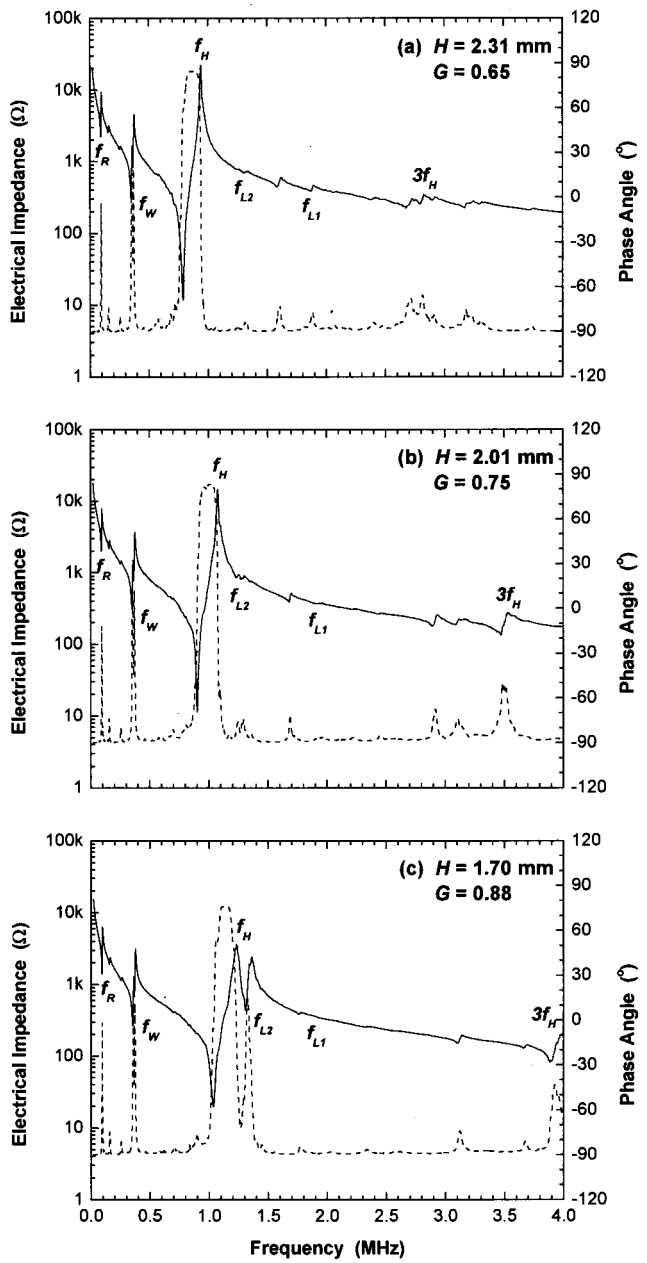

FIG. 6. Electrical impedance (solid line) and phase angle (dot line) versus frequency plots for composite ring with $\phi = 0.91$ and $L = 1.50$ mm at different thicknesses are shown.

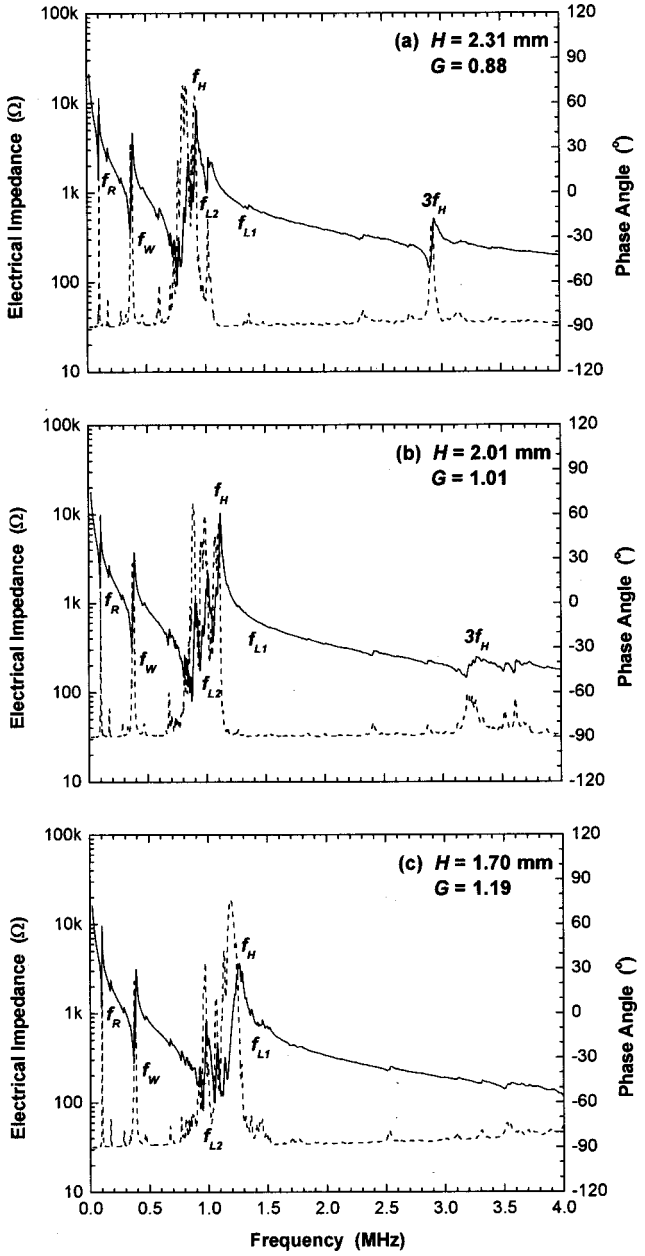

FIG. 7. Electrical impedance (solid line) and phase angle (dot line) versus frequency plots for composite ring with $\phi = 0.94$ and $L = 2.03$ mm at different thicknesses are shown.

because the PZT used in the present study has strong lateral coupling. For ultrasonic wire bonding transducer applications, piezoelectric rings with thicknesses of less than 1 mm are seldom used as they are susceptible to breakage during fabrication. Therefore, f_{L2} acts as an upper frequency bound for the operation of f_H, in practice.

B. Cooperative resonances of composite rings

1. Radial and wall-thickness mode resonances

f_R and f_W are the two low frequency resonance modes in a thin ring resonator as shown in Figs. 2–7. The several weak resonances following f_R and f_W are their harmonics. They have frequencies approximately equal to an integral multiple of them. Due to the mechanical absorption of the epoxy matrix, both f_R and f_W become weaker in comparison with the pure PZT ring (Fig. 9). So, it is an advantage to use 1–3 composites instead of PZT in order to fabricate transducers with low lateral mode-coupling characteristics.

As shown in Fig. 10, the observed f_R and f_W taken at the series resonance frequency decrease slightly as the ring thickness increases but increase as ϕ increases. The dependence of f_R and f_W on ϕ elucidates the existence of different degrees of lateral clamping of the PZT elements by the epoxy matrix at different ϕ. If the composite ring thickness becomes comparable to its wall thickness (3.85 mm), f_H will couple with f_W. Hence, f_W acts as a lower frequency bound, which limits the selection of the thickness of the ring.

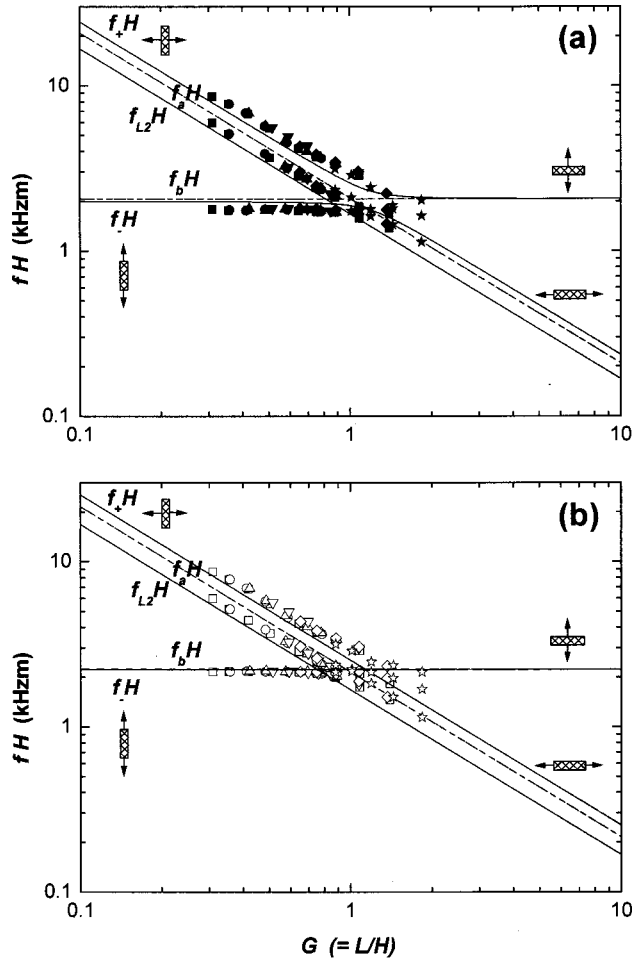

FIG. 8. Log–log plots of resonance frequency times element height fH versus configuration ratio G $(=L/H)$ for PKI804 elements with square cross section under (a) short- and (b) open-circuit conditions are shown. The lines and symbols represent the theoretical and experimental results, respectively. The squares, circles, up triangles, down triangles, diamonds, and stars are the experimental results for composite rings with $\phi=0.82$, 0.84, 0.87, 0.89, 0.91, and 0.94, respectively.

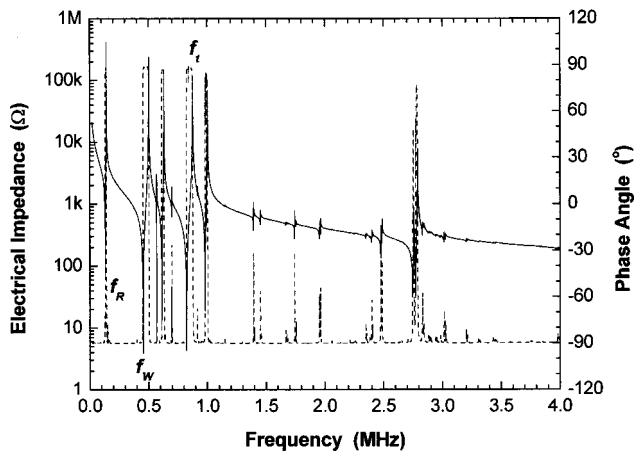

FIG. 9. Electrical impedance (solid line) and phase angle (dot line) versus frequency plot for a PKI804 PZT ring with an outer diameter, an inner diameter, and a thickness of 12.7 mm, 5.0 mm, and 2.5 mm, respectively, are shown.

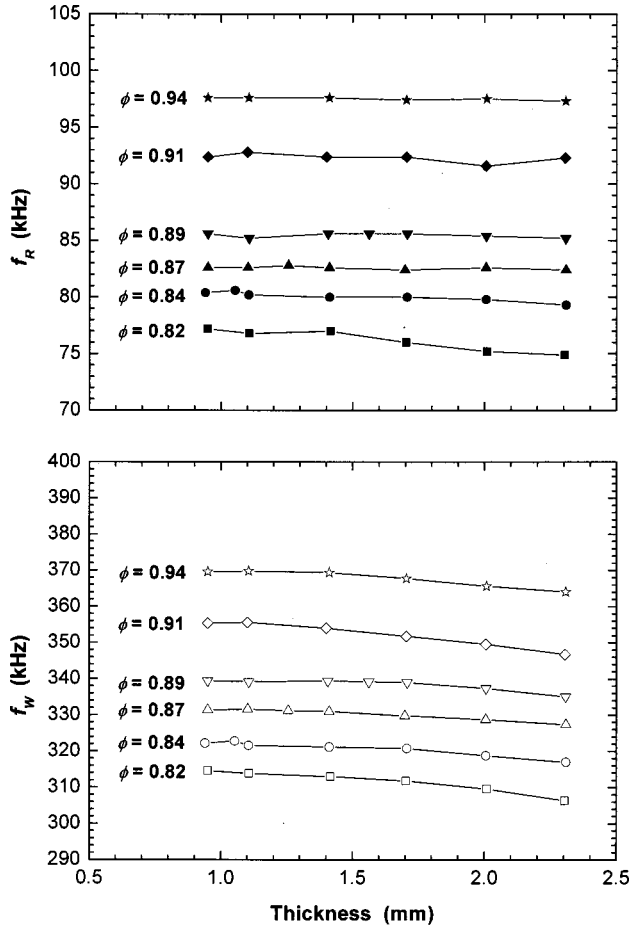

FIG. 10. Variation of radial f_R and wall-thickness f_W mode resonance frequencies with sample thickness for composite rings at different PZT volume fractions ϕ is shown.

2. Stopband resonances

The empirical resonance frequency equations proposed by Geng *et al.*[18] were employed to estimate the two lateral stopband resonances f_{S1} and f_{S2}. They are given as follows:

$$f_{S1}=\frac{f_{S2}}{\sqrt{2}}, \tag{8}$$

$$f_{S2}=\frac{v_s}{2d_P}, \tag{9}$$

where f_{S2} can be viewed as a half-wave resonance in the epoxy gap width d_P while f_{S1} can be considered as another half-wave resonance across the diagonal direction $\sqrt{2}d_P$, and v_S denotes the shear wave velocity in the epoxy.

Using $v_S=1207$ m/s for Araldite LY5210/HY2954 epoxy,[13] f_{S1} and f_{S2} were calculated to be 5.54 MHz and 7.84 MHz, respectively. However, an investigation into the electrical impedance spectra for frequencies up to 10 MHz found no observable resonance peaks for all the samples studied. The reasons are probably that the PZT elements are much larger than the epoxy gap width and are spaced so closely that the possible reflection of shear waves is weakened and the resulting standing waves cannot be greatly enhanced in this limited epoxy gap width.

VII. CONCLUSION

PKI804/Araldite LY5210/HY2954 1–3 piezocomposite rings with ϕ varying from 0.82 to 0.94 have been fabricated, and their resonance characteristics have been studied theoretically and experimentally to elucidate the mode-coupling behavior. These composite rings have sufficiently small epoxy width ($\sim$77 μm) and can be treated as an effective homogeneous medium in which f_{S1} and f_{S2} are not observed. f_H has been found to increase linearly with the decrease in element height while f_{L1} and f_{L2} remained quite stable. f_R and f_W have been observed to be independent of ring thickness but increased as ϕ increases. In designing a transducer for ultrasonic wire bonding, for example, in addition to optimizing the homogeneity, material properties, and manufacturing cost of the composite rings, one should also avoid other resonance modes being coupled to f_H. This in turn requires a ring thickness not too thin in order to keep f_H smaller than all lateral modes of the PZT elements ($G < 0.8$) but not too thick to avoid coupling of f_H with f_W and f_R of the ring. Based on the current findings, an optimal set of composite rings has been obtained and used in the development of various ultrasonic wire bonding transducers with low mode coupling and wide bandwidth. Details are reported in separated articles.[13–16]

ACKNOWLEDGMENTS

Financial support from the Innovation and Technology Fund (ITF UIM/29), the Centre for Smart Materials of The Hong Kong Polytechnic University, and ASM Assembly Automation Ltd. are acknowledged.

[1] R. E. Newnham, D. P. Skinner, and L. E. Cross, Mater. Res. Bull. **13**, 525 (1978).
[2] W. A. Smith and B. A. Auld, IEEE Trans. Ultrason. Ferroelectr. Freq. Control **38**, 40 (1991).
[3] G. Hayward, J. Bennett, and R. Hamilton, J. Acoust. Soc. Am. **98**, 2187 (1995).
[4] W. A. Smith, A. Shaulov, and B. A. Auld, Proceedings of the 1985 IEEE Ultrasonics Symposium, San Francisco, CA, October 1985, p. 642.
[5] T. R. Gururaja, W. A. Schulze, L. E. Cross, R. E. Newnham, B. A. Auld, and Y. J. Wang, IEEE Trans. Ultrason. Ferroelectr. Freq. Control **32**, 481 (1985).
[6] T. R. Gururaja, W. A. Schulze, L. E. Cross, and R. E. Newnham, IEEE Trans. Sonics Ultrason. **32**, 499 (1985).
[7] H. L. W. Chan, Ph.D. Thesis, Macquarie University, 1987.
[8] H. L. W. Chan and J. Unsworth, J. Appl. Phys. **65**, 1754 (1989).
[9] J. A. Hossack and G. Hayward, IEEE Trans. Ultrason. Ferroelectr. Freq. Control **38**, 618 (1991).
[10] G. Hayward and J. Bennett, IEEE Trans. Ultrason. Ferroelectr. Freq. Control **43**, 98 (1996).
[11] Q. M. Zhang, W. Cao, H. Wang, and L. E. Cross, J. Appl. Phys. **73**, 1403 (1993).
[12] H. L. Li, H. L. W. Chan, and C. L. Choy, Proceedings of the Third Asian Meeting on Ferroelectrics, Hong Kong, China, December 2000 (in press).
[13] S. W. Or, Ph.D. Thesis, The Hong Kong Polytechnic University, 2001.
[14] H. L. W. Chan, S. W. Or, K. C. Cheng, and C. L. Choy, U.S. Patent, No. US6, 190, 497, B1 (2001).
[15] S. W. Or, H. L. W. Chan, and Y. M. Cheung, Proceedings of the 2001 Annual International Conference on Advanced Ceramics and Composites, Cocoa Beach, FL, January 2001 (in press).
[16] S. W. Or and H. L. W. Chan, IEEE Trans. Ultrason. Ferroelectr. Freq. Control (in press).
[17] S. W. Or and H. L. W. Chan, Proceedings of the Third Asian Meeting on Ferroelectrics, Hong Kong, China, December 2000 (in press).
[18] X. Geng and Q. M. Zhang, J. Appl. Phys. **85**, 1342 (1999).
[19] *Performance Ceramics Data Book* (Piezo Kinetics, Incorporated, Philadelphia, PA, 1999).